

RAPID CALCULATION OF PROPAGATION PATH INFORMATION BY APPLICATION OF THE METHOD OF IMAGES

Garry J. Heard

Defence Research Establishment Pacific,
FMO Victoria, B.C.,
Canada, V0S 1B0

ABSTRACT

Many problems in underwater acoustics require rapid computation of acoustic path information. Inversions that employ simulated annealing and Monte Carlo minimization techniques may require the computation of millions of acoustic paths for application to a problem. This paper describes the application of the method of images for rapidly computing propagation path lengths, time differences, and other path details between an acoustic source and a receiving hydrophone in a uniformly sloping ocean environment. The problem is kept simple by considering only a constant sound-speed profile. This assumption limits the applicability of the method. To test the accuracy of the method, expressions for the error are developed for a particular environment that represents a severe case. The constant-sound-speed calculations are shown to result in sufficient accuracy that they may be applied to short-range, steep-angle propagation problems.

SOMMAIRE

Beaucoup de problèmes dans le domaine de l'acoustique sousmarine exigent le calcul rapide d'informations portant sur les trajets acoustiques. Les inversions qui emploient des techniques de recuit simulé et de la minimalisation de Monte Carlo peuvent nécessiter le calcul de millions de trajets acoustiques pour qu'elles s'appliquent à un problème. Dans cette étude nous décrivons l'application de la méthode d'images pour le calcul rapide de longueurs des trajets de propagation, des différences temporelles et d'autres détails concernant les trajets entre une source acoustique et un hydrophone de réception dans un environnement océanique à pente uniforme. Nous facilitons le problème en ne considérant qu'un profil de vitesse du son constante. Cette supposition limite l'applicabilité de la méthode. Afin d'éprouver l'exactitude de la méthode, des expressions pour l'erreur sont développées visant un environnement particulier qui représente un cas sévère. Nous démontrons que les calculs utilisant une vitesse du son constante ont pour résultat une exactitude suffisante pour que l'on puisse les appliquer aux problèmes de propagation de portée courte et d'angle raide.

1 INTRODUCTION

The solution of an acoustic problem may require the determination of acoustic propagation path details for thousands to millions of separate ray-paths. A specific example is the determination of an array's location from propagation time differences. The array's location can be determined by minimizing cost functions whose independent variables are the measured time differences for different propagation paths. Problems of this kind may be solved using simulated annealing and Monte Carlo

minimization techniques[1]. Such problems require efficient path determination algorithms to allow the solution to be attained in a reasonable time period. When dealing with this kind of problem there is strong motivation to reduce the complexity of the acoustic modelling and, hence, reduce the computation overhead. This paper describes one method of reducing the computational load in determining acoustic path details such as path length, grazing angle, and range to bottom and surface interactions. The method described is the *Method of Images* and in the current form is applicable to two-

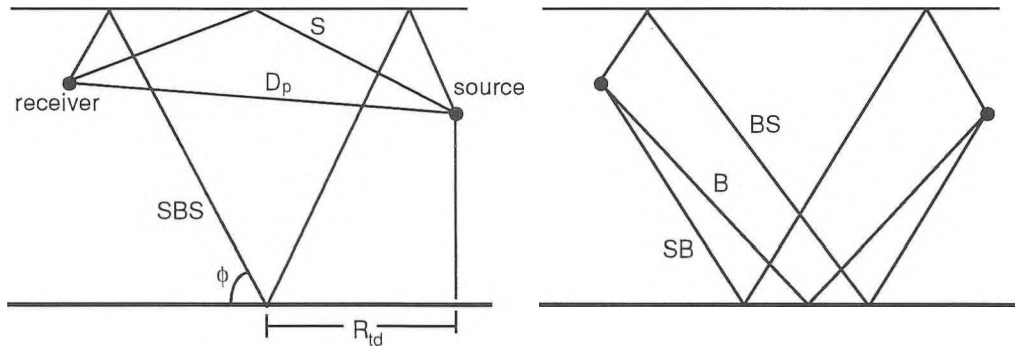


Figure 1: Definition of the primary paths of the acoustic signature.

dimensional problems with uniformly shelving sea-floor. The method described could handle three-dimensional problems with inclined flat bottoms, but extensions of this kind are not considered in this paper. The method implicitly assumes that the ocean sound-speed is constant, so that ray paths can be represented by straight lines. This constant-sound-speed approximation results in a degree of error that generally limits the use of the method to problems involving short-range, steep-angle propagation.

The following section defines the path names and variables, and describes an ocean environment which has a smooth sea-floor that may be inclined with respect to the ocean surface. In Section 3 equations are developed for the apparent source or receiver position in terms of matrix operators that are easily implemented on digital computers. Path parameters are extracted from the position vectors and the errors in using the method of images as opposed to a more accurate ray-tracing scheme are investigated. In Section 4 the method is applied to the interpretation of a marine seismic data stack. Finally, in Section 5 the application and limitations of the method are summarized.

2 PROBLEM DEFINITION

The primary acoustic paths between a source and receiver include the direct, bottom-bounce, and surface-bottom interactions. These paths are denoted by D_p , S , B , SB , BS , and SBS as defined in Fig. 1. The goal of this note is to develop equations for computing the path lengths, propagation times, and other details of these primary acoustic paths. Higher orders of bottom bounces are possible in practice and the equations developed here can be used to determine the details associated with them. In general it will be found that the method is limited to short ranges, and therefore most directly applicable to the primary paths.

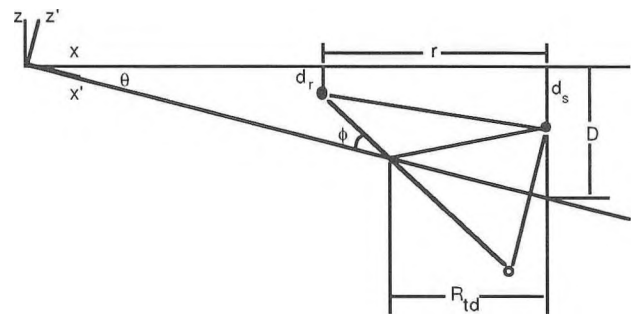


Figure 2: Geometry of the problem. The ocean bottom is assumed to be uniformly sloping at angle θ with respect to the horizontal.

Figure 2 shows the geometry of the problem. The source is located on the right-hand side of the figure and the receiver on the left. This figure also defines the symbols used in this note. To be specific, d_s is the depth of the source, d_r is the depth of the receiver, and D is the depth of the ocean at the source location. The symbol r is used to denote the horizontal range between the source and the receiver, while R_{td} denotes the horizontal range to the point where the ray *touches down*. The ocean bottom makes an angle θ with the horizontal and the angle ϕ is the grazing angle with respect to the ocean bottom. In the next section, expressions are developed to determine the path lengths, the propagation times, the grazing angle ϕ , and the range to the touch-down point R_{td} .

3 EQUATION DEVELOPMENT

The coordinate system (x, z) is relative to the ocean surface and the system (x', z') is relative to the ocean bottom. In both systems, z is positive in the upward

direction. The ocean-bottom coordinate system can be obtained from the ocean-surface coordinate system by a simple rotation of angle θ about the origin. The transformation from the unprimed to the primed coordinate system is

$$\vec{P}' = \begin{pmatrix} x' \\ z' \end{pmatrix} = \mathbf{T} \cdot \vec{P} = \begin{pmatrix} \cos(\theta) & -\sin(\theta) \\ \sin(\theta) & \cos(\theta) \end{pmatrix} \cdot \begin{pmatrix} x \\ z \end{pmatrix} \quad (1)$$

In order to calculate the acoustic path details using the method of images it is necessary to determine the apparent coordinates of an image of the source and the coordinates of the receiver in the same reference system. The path length and grazing angle are then easily determined from the difference in the coordinates. Similarly, the range to a boundary interaction can be determined from the difference in the coordinates of the source (or receiver) and the coordinates of the touch-down point Q.

To see how this method is applied, consider for the moment path B. We begin by determining the position vectors for the source and receiver. Eq.(1) is then used to transform these position vectors to the ocean bottom reference system.

Referring to Fig. 2 we can see that the source location vector in the surface coordinate system is

$$\vec{P}_s = (x_s, z_s)^\dagger = (D/\tan(\theta), -d_s)^\dagger \quad (2)$$

(where the \dagger denotes the transpose of the vector). Similarly, the receiver location vector is

$$\vec{P}_r = (x_r, z_r)^\dagger = (D/\tan(\theta) - r, -d_r)^\dagger \quad (3)$$

Using Eq.(1) we obtain the location vectors in the ocean-bottom coordinate system

$$\vec{P}'_s = \mathbf{T} \cdot \vec{P}_s \quad (4)$$

and

$$\vec{P}'_r = \mathbf{T} \cdot \vec{P}_r \quad (5)$$

Once these are known, we need to find the location of the source image in the ocean bottom.

A matrix imaging operator is easily determined by noting that if the source is located at $(x'_s, z'_s)^\dagger$, then the image of the source is located at $(x'_s, -z'_s)^\dagger$. The matrix operator that performs this transformation is

$$\mathbf{M} = \begin{pmatrix} 1 & 0 \\ 0 & -1 \end{pmatrix} \quad (6)$$

If \vec{P}'_s is the position of the source with respect to the bottom coordinate system, then

$$\vec{P}'_{sB} = \mathbf{M} \cdot \vec{P}'_s = \mathbf{M} \cdot \mathbf{T} \cdot \vec{P}_s \quad (7)$$

is the position of the image of the source in the bottom coordinate system. The path length is then given by Pythagoras' theorem as

$$L = \sqrt{(\vec{P}'_{sB} - \vec{P}'_r)^\dagger \cdot (\vec{P}'_{sB} - \vec{P}'_r)} \quad (8)$$

The travel time is then just

$$t = \frac{L}{c} \quad (9)$$

where c is the speed of sound.

Consider now path S. For this path the imaging operation occurs at the ocean surface and it is not necessary to transform the locations to the ocean-bottom coordinate system. We merely find the image of the source in the surface and apply Pythagoras' theorem:

$$\vec{P}_{sS} = \mathbf{M} \cdot \vec{P}_s \quad (10)$$

and

$$L = \sqrt{(\vec{P}_{sS} - \vec{P}_r)^\dagger \cdot (\vec{P}_{sS} - \vec{P}_r)} \quad (11)$$

By combining the procedures for a surface and bottom reflection in the proper order, it is possible to compute the apparent source position for any number of surface and bottom reflections. For path SB the sequence of operations is

$$\vec{P}'_{sSB} = \mathbf{M} \cdot \mathbf{T} \cdot \mathbf{M} \cdot \vec{P}_s \quad (12)$$

For path BS the bottom imaging is done before the surface imaging. The sequence of operations would be

$$\vec{P}'_{sBS} = \mathbf{T} \cdot \mathbf{M} \cdot \mathbf{T}^{-1} \cdot \mathbf{M} \cdot \mathbf{T} \cdot \vec{P}_s \quad (13)$$

For path SBS the sequence of operations would be

$$\vec{P}'_{sSBS} = \mathbf{T} \cdot \mathbf{M} \cdot \mathbf{T}^{-1} \cdot \mathbf{M} \cdot \mathbf{T} \cdot \mathbf{M} \cdot \vec{P}_s \quad (14)$$

This application of imaging and rotation operators can be repeated indefinitely to obtain the apparent source position for paths with any number of bottom bounces. The path lengths and propagation times are then found by substitution for \vec{P}'_{sB} in Eq.(8) and application of Eq.(9).

For those paths (B, SB, SBSB, etc.) that interact with the bottom immediately before reception at the receiver, the grazing angle ϕ at the last bottom interaction is determined from

$$\phi = \arctan \left(\frac{z'_s + z'_r}{x'_s - x'_r} \right) \quad (15)$$

where the x' and z' are the apparent ocean-bottom coordinates that result from the application of an appropriate sequence of imaging and rotation operators. For those paths that last interact with the surface (S, BS, etc.),

the last surface grazing angle can be determined using Eq.(15) with ocean-surface coordinates substituted for the primed x and z coordinates. The determination of grazing angles at earlier boundary interactions can be done by applying operators to both the source and receiver and working toward the interaction point, Q , that is of interest.

For path B, the position of the touch-down point, Q , in the ocean-bottom coordinate system is

$$\vec{Q}' = \left(x'_s - \frac{z'_s}{\tan(\phi)}, 0 \right)^\dagger \quad (16)$$

This vector can be transformed to the ocean-surface coordinate system to obtain the touch-down range and the water depth at that range

$$R_{td} = x_s - x_Q \quad (17)$$

and

$$D_{td} = -z_Q \quad (18)$$

The touch-down range for more complicated paths is obtained by working toward the interaction region of interest, at point Q , from both the source and receiver. An intermediate position vector \vec{q}' is then determined from the apparent source image location and the grazing angle. The vector \vec{Q} is obtained by transforming the intermediate result to the ocean-surface coordinate system, and the difference between the x -components of the actual source position and the apparent image source position is added to x -component of \vec{q} . This addition to the x -component is necessary because each bottom interaction has the effect of moving the apparent source position closer to the origin. Eq.(18) can then be used to obtain the touch-down range and the water depth at that range.

In order to determine the limit of applicability of the iso-speed assumption an expression has been developed for the difference between the touch-down range from a straight ray path geometry and the touch-down range determined by ray-tracing [2]. A second expression was developed for the difference in the grazing angles. Both of these expressions were developed for the case of the source located at the surface of the ocean and for a horizontal ocean bottom.

Telford [2] gives the range to the touch-down point as

$$X(p) = \int_{d_s=0}^D \frac{pV(z)}{\sqrt{1-p^2V(z)^2}} dz \quad (19)$$

where p is the ray parameter $p = \sin \theta / V(z_s)$ (θ here is the angle of incidence), $V(z)$ is the sound speed, and z is the depth. The range to the touch-down point for

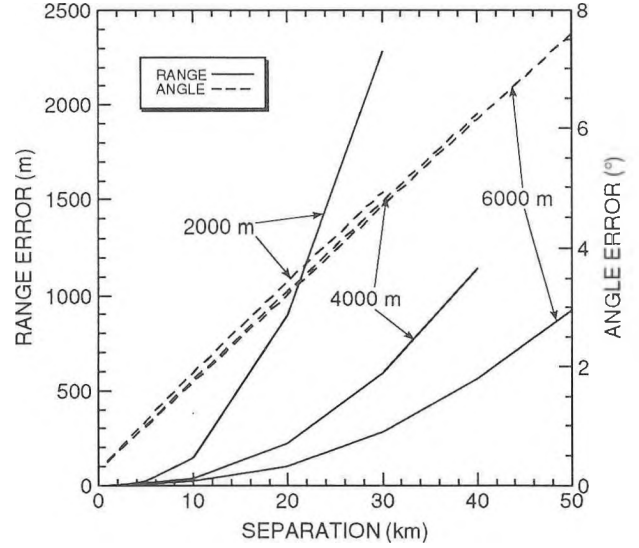


Figure 3: Error versus source-receiver separation for an idealized Arctic sound-speed profile.

a constant sound-speed environment with the source at the surface and a horizontal bottom is

$$R_{td} = Dr / (2D - d_r) \quad (20)$$

So the range error in using the straight line approximation is

$$E_{td} = R_{td} - X(p) \quad (21)$$

where p , the ray parameter must be determined for the eigenray of interest. The quantity E_{td} must in general be evaluated numerically for a particular sound-speed profile. An illustrative case is obtained when $V(z)$ is a linear profile that could represent an idealized Arctic sound-speed profile. Such an environment is a severe case, since upward refraction occurs at all locations within the water column. Typical sofar channel environments tend to result in less error for shallow sources, because the ray paths undergo an inflection. If $V(z) = az + b$, then $X(p)$ can be evaluated analytically

$$X(p) = \frac{\sqrt{1-b^2p^2}}{ap} - \frac{\sqrt{1-b^2p^2-2abDp^2-a^2D^2p^2}}{ap} \quad (22)$$

where for an Arctic profile $a = 0.0164$ and $b = 1450$ (note that if $a = 0$, then the sound-speed is constant and Eq.(19) reduces to Eq.(20) resulting, as it should, in $E_{td} = 0$).

In similar fashion, the grazing angle for the ray-tracing case is $\phi(p) = 90 - \arccos \sqrt{1-p^2V(D)^2}$ and for the constant sound-speed case the grazing angle is $\gamma = \arctan \frac{2D-d_r}{r}$. The error in grazing angle is given

by the difference

$$E_\phi = \gamma - \phi \quad (23)$$

Figure 3 shows the errors in range and grazing angle with the idealized Arctic sound-speed profile for 2000, 4000, and 6000 m ocean depths. In all three cases the source is located at the surface and the receiver is at 1000 m depth. Range errors are seen to grow more rapidly as the source-receiver separation is increased. The steeper the angle of propagation the smaller the range error becomes. If a 200 m range error can be tolerated, then it is seen that the maximum allowable source-receiver separation goes from 11–26 km as the ocean depth is increased from 2000–6000 m under the current conditions. For many practical sound-speed profiles greater ranges will be permissible. Angle error is seen to increase almost linearly with source-receiver separation and is almost independent of the ocean depth.

4 AN EXAMPLE

A simple example is now given that illustrates the use of the method of images. Real data, collected during the WEDGEX experiment [3], is compared with the results from a signal arrival-time model based on the equations of the last section. The model calculates the time of flight from a source location to 32 receiver locations for the four components of the single bottom-bounce group of arrivals. The model implicitly incorporates dynamic moveout adjustments due to the different receiving hydrophone locations.

Figure 4 shows a marine-seismic stack of filtered data from the WEDGEX experiment carried out over the continental slope off the west coast of Vancouver Island. Modelled arrival times for the four components of the first bottom-bounce group are overlaid as dashed lines. In the example shown, agreement between the model and real data is not exact, but it is sufficient to show that the mean water depth in the bottom interaction region was approximately 1500 m and that the mean bottom-slope was 4° with depth increasing with range. This bathymetry is the opposite of what was expected and appears to be due to the presence of a shallow underwater canyon. In addition, source-receiver separation information can be obtained from the comparison, and the model serves as an interpretation aid by easing the identification of the surface interacting components.

With the development of appropriate cost functions measuring the differences between the real arrival times and the modelled results, the example given here suggests that the method of images would be useful in optimization techniques, such as simulated annealing, for determining the structure and properties of the sea floor. In such a problem involving hundreds of thousands of

ray-path computations, the method of images represents a considerable saving in computation time over more exact procedures.

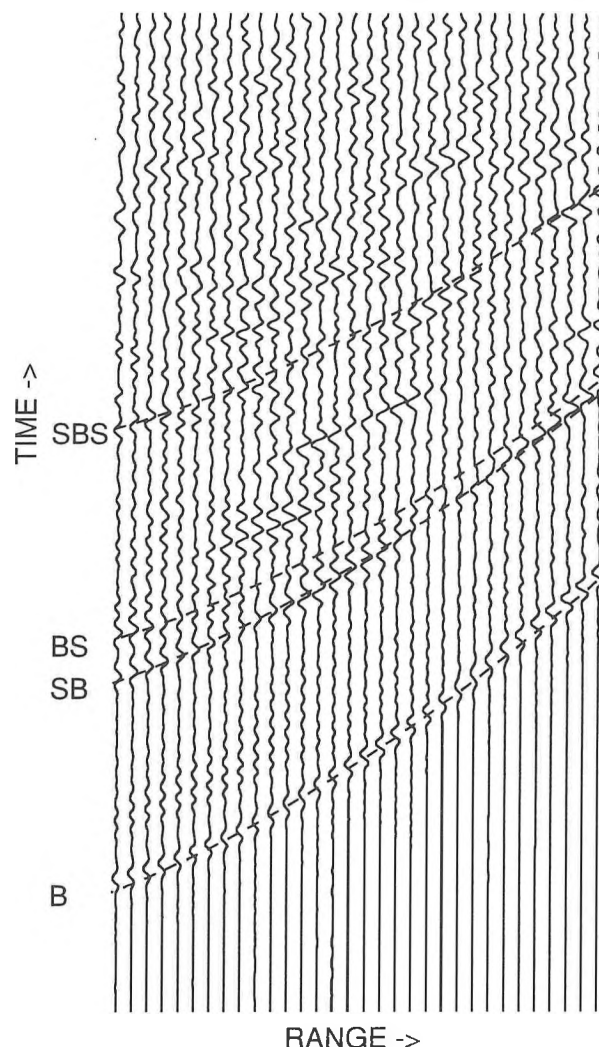


Figure 4: Comparison of a marine-seismic stack and modelled arrival times based on the equations developed in the last section. Vertical traces are from hydrophones separated by 38.1 m and represent about 1.3 seconds of data.

5 SUMMARY

In Section 3 equations describing the details of various ray-paths were developed for an iso-speed environment. The iso-speed assumption greatly simplifies the development of the equations and results in simple formulae that are particularly suited to implementation on a computer. The simplicity and the fixed rules for handling bottom and surface interactions result in fast com-

putation times that are highly desirable for problems involving many path determinations. The constant sound-speed simplification limits the application of the equations in practical situations. Expressions were developed for the errors in range and grazing angle for an environment with monotonic upward refraction that represents a severe case. The results indicate that the method of images can be used to simplify the solution of certain acoustic problems subject to a range limitation based on the allowable errors. In many practical problems where range errors of several hundred meters and a few degrees are acceptable, the method is applicable at ranges exceeding 10 km.

REFERENCES

- [1] M.D. Collins, W.A. Kuperman, H. Schmidt, "Nonlinear inversion for ocean-bottom properties," *J. Acoust. Soc. Am.*, **92**(5), p.2770-2784, (1992).
- [2] V.M. Telford, L.P. Geldart, R.E. Sheriff, D.A. Keys, "Applied Geophysics," Cambridge University Press (1976).
- [3] G.J. Heard, D.J. Thomson, G.H. Brooke, "Upslope propagation data versus two-way PE," Proceedings of the Ocean Reverberation Symposium, 25-29 May 1992, Kluwer Press.

INCREDIBLE VERSATILITY

At Only 2.2 lbs.



Rion's new NA-29 provides unusual capabilities for a pocket-size acoustical analyzer weighing only 2.2 lbs. It's displays include:

- Lmax, Ln, Lavg, Leq.
- Sound level in large digits.
- Real-time octave analysis centered 31.5 Hz. through 8000 Hz.
- Level vs. time, each frequency band.
- 1500 stored levels or spectra.
- Spectrum comparisons.

It also features external triggering, AC/DC outputs, and RS-232C I/O port. A preset processor adds additional versatility for room acoustics and HVAC applications. To minimize external note taking, users can input pertinent comments for each data address. Specify the NA-29E for Type 1 performance or the NA-29 for Type 2.

Our combined distribution of Norwegian Electronics and Rion Company enables us to serve you with the broadest line of microphones, sound and vibration meters, RTAs, FFTs, graphic recorders, sound sources, spectrum shapers, multiplexers, and room acoustics analyzers, plus specialized software for architectural, industrial and environmental acoustics. You'll also receive *full service*, warranty and application engineering support. Prepare for the '90s.

SCANTEK INC.
Norwegian Electronics • Rion

Call today. (301) 495-7738

916 Gist Avenue • Silver Spring, MD 20910